Excitons in atomically thin black phosphorus

A. Surrente,[1] A. A. Mitioglu,[1,2,*] K. Galkowski,[1] W. Tabis,[1,3] D. K. Maude,[1] and P. Plochocka[1,†]

[1] *Laboratoire National des Champs Magnétiques Intenses, UPR 3228, CNRS-UJF-UPS-INSA, Grenoble and Toulouse, France*
[2] *Institute of Applied Physics, Academiei Str. 5, Chisinau, MD-2028, Republic of Moldova*
[3] *AGH University of Science and Technology, Faculty of Physics and Applied Computer Science, Al. Mickiewicza 30, 30-059 Krakow, Poland*

(Dated: January 7, 2016)

Raman scattering and photoluminescence spectroscopy are used to investigate the optical properties of single layer black phosphorus obtained by mechanical exfoliation of bulk crystals under an argon atmosphere. The Raman spectroscopy, performed in situ on the same flake as the photoluminescence measurements, demonstrates the single layer character of the investigated samples. The emission spectra, dominated by excitonic effects, display the expected in plane anisotropy. The emission energy depends on the type of substrate on which the flake is placed due to the different dielectric screening. Finally, the blue shift of the emission with increasing temperature is well described using a two oscillator model for the temperature dependence of the band gap.

Black phosphorus, the most stable of all the allotropes of phosphorus, has been intensively studied by different experimental methods from the early fifties of the last century.[1–7] Bulk black phosphorus is a semiconductor, with a band gap of about 0.335 eV.[1,4] The orthorombic bulk crystal has a layered structure, with atomic layers bound by weak van der Waals interactions. A single atomic layer is puckered, with the phosphorous atoms being parallel in the (010) plane.[3,8,9] Atomically thin monolayers have been recently isolated using mechanical exfoliation,[10] adding black phosphorus to the rapidly growing family of emerging two dimensional materials. The band gap of black phosphorus is always direct and can be tuned from 0.3 eV to the nearly visible part of the spectrum[11,12]. In contrast, graphene is gapless,[13] and the transition metals dichalcogenides (TMDs) have an indirect gap in bulk phase and only monolayer TMDs have a direct gap.[14] Moreover, black phosphorus exhibits a strong in-plane anisotropy[11,12,15–17], absent in graphene and TMDs. Additionally, the relatively high mobilities measured at room temperature combined with the direct band gap result in an on/off ratio for FET transistors of the order of 10^5.[12,18,19]

Although black phosphorus has a wide range of possible applications, including tunable photodetectors[20], field effect transistors[12,16,18,19] or photon polarizers[11,12,15–17], many of its electronic properties are not yet fully understood. The main difficulty arises from the sensitivity of black phosphorus to its environment, notably its high reactivity when exposed to air and laser light.[10,21,22] Theoretical calculations predict a band gap of few layer black phosphorus ranging from 1 eV[11,19] to 2.15 eV[10,11], with a binding energy of the neutral exciton of 0.8 eV in vacuum[11] and of 0.38 eV when placed on a Si/SiO_2 substrate[10]. The measured photoluminescence (PL) emission energy from bi-layers black phosphorus is between 1.2 eV[23] and 1.6 eV[10], while monolayer black phosphorus shows neutral exciton emission around 1.3 eV[24], 1.45 eV[19] or 1.76 eV[25]. The latter value was related to the simultaneous observation of charged exciton emission at around 1.62 eV.[25] Using scanning tunneling microscopy the band gap of a single layer of black phosphorus was estimated to be 2.05 eV.[26] The exciton binding energy and consequently the emission energy strongly depend on the dielectric environment (substrate)[10,27]. This could partially explain the wide range of values for the black phosphorus emission energy found in the literature, possibly related also to a slightly different composition of the SiO_2 substrates employed. Moreover, owing to the limited life time of the samples, the various characterization techniques used to identify monolayer black phosphorus (*e.g.* atomic force microscopy, Raman spectroscopy) could not always be performed *on the same flake* where the optical response was investigated.

In this paper we present a systematic investigation of the optical properties of monolayer of black phosphorus. We analyze the properties of the emission as a function of the dielectric constant of the substrate, excitation power, polarization and temperature. The single layer character of the investigated flakes is demonstrated using *in situ* Raman measurements on the same flake used for the PL. We show that the PL emission energy of monolayer black phosphorus depends on the substrate used. The PL spectra, dominated by excitonic effects, exhibit the expected in plane anisotropy. Finally, the blue shift of the emission energy with an increasing temperature is well described with a two-oscillator model for the temperature dependence of the band gap.

Single and few layer black phosphorus flakes have been obtained by mechanical exfoliation of a bulk crystal, purchased from Smart Elements (99.998% nominal purity). The mechanical exfoliation was performed in a glove box filled with argon (Ar) gas (< 1 ppm O_2, < 1 ppm H_2O). The flakes were subsequently transferred onto a Si substrate, in most cases capped with a 300 nm thick layer of SiO_2 (Si/SiO_2 hereafter). The samples were stored in vials, in the glove box, before their transfer to the cryostat under an Ar atmosphere.

For the optical measurements, the samples were

mounted on the cold finger of a He-flow cryostat, which was then rapidly pumped to a pressure below 1×10^{-4} mbar, minimizing the exposure of the black phosphorus to air. The excitation was provided by a frequency-doubled diode laser, emitting at 532 nm and focused on the sample by a 50× microscope objective (0.55 numerical aperture), yielding a spot size of $\sim 1\,\mu$m. The PL and Raman signals were collected through the same objective and analyzed by a spectrometer equipped with a liquid nitrogen cooled Si CCD camera.

Raman spectroscopy, which has been shown to be a very precise tool for the determination of the number of layers in TMDs[14,28–31] and in graphene,[32,33] can also be used to identify monolayer black phosphorus. Bulk black phosphorus belongs to the D_{2h}^{18} space group. Of the 12 normal modes at the Γ point of the Brillouin zone, six are Raman active.[7,34] The two B_{3g} modes are forbidden in back scattering configuration and the B_{1g} mode at 194 cm^{-1} is very weak. Therefore, only three Raman modes are expected for bulk black phosphorus: A_g^1, A_g^2 and B_{2g} at around 365 cm^{-1}, 470 cm^{-1} and 442 cm^{-1}, respectively.[7,34] The A_g^2 and B_{2g} modes are related to the in plane vibrations of the atoms, while A_g^1 mode is related to the out of plane movement of the atoms[7,34].

Typical calibrated micro Raman (μRaman) spectra of the bulk and single layer black phosphorus are presented in Fig. 1. For the bulk crystal three strong peaks are observed at 363.7 cm^{-1}, 440.3 cm^{-1} and 467.5 cm^{-1} corresponding well to the expected main Raman modes. A further peak was systematically observed at 520 cm^{-1} (Raman mode of the Si substrate, not shown here), confirming the correct calibration of our Raman setup. The slight shift towards lower frequencies can be related to the low temperature (4 K) at which our measurements have been carried out, which shifts the characteristic Raman features towards lower frequencies[23]. Under low excitation power (17 μW), initially used to avoid any risk of inducing damage by exposure to the laser light, the Raman spectrum of the monolayer flake is similar to that of the bulk crystal. This suggests that the monolayer black phosphorus remains crystalline and no oxidization occurred during the transfer of the sample from the glove box to the cryostat. Compared to bulk, the A_g^1 mode does not shift within experimental error. In contrast, the position of A_g^2 and B_{2g} Raman modes shift to higher frequencies in the monolayer flake. The A_g^2 mode shifts by 1.7±0.2 cm^{-1} while the B_{2g} shifts by 1.0±0.2 cm^{-1}. The change of the energy of the Raman modes as a function of the number of layers in black phosphorus has been already shown for both high[10,19,35] and low frequency modes[36]. The shifts we measure are in good agreement with the reported values for single layer black phosphorus (~ 1.9 cm^{-1} and between ~ 1.0 cm^{-1} and ~ 1.6 cm^{-1} for A_g^2[10,19,35,37] and B_{2g}[10,35], respectively) demonstrating the single layer character of the investigated flake. Raman measured at high excitation power (260 μW, the same as used for the bulk crystal) does not show any additional features; the peak positions remain the same as for the data obtained for low excitation power. Thus there is no sign of laser induced chemical modification of our samples,[10] which is important since the excitation intensity used here is comparable to that used in our micro PL (μPL) spectroscopy measurements.

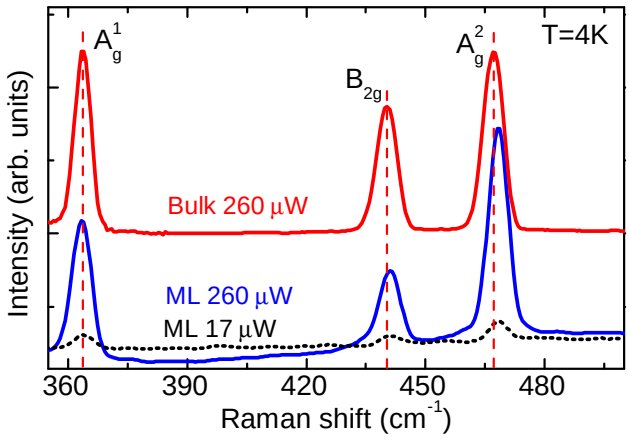

FIG. 1. (Color online) Typical μRaman spectra of bulk and single layer black phosphorus measured at $T = 4$ K for different excitation powers as indicated. The dashed lines indicate the position of the three Raman modes A_g^1, A_g^2 and B_{2g} in bulk black phosphorus.

In Fig. 2(a) we show representative low temperature μPL spectra for the monolayer flake previously characterized using Raman spectroscopy. The measurement was performed without removing the flake from the cryostat, which was maintained under vacuum. The spectrum is dominated by a very strong emission line centered at around 2 eV identified with neutral exciton recombination. This line is consistently observed at this energy for all flakes transferred to Si/SiO_2 substrates. The typical full width at half maximum is of $\lesssim 90$ meV (line broadening induced by scattering with vacancies and impurities in the exfoliated flakes). The observed value of the exciton recombination energy is relatively high as compared to the theoretical band gap of 2.15 eV computed for black phosphorus single layer[10,11] and is somewhat larger than the values already reported for black phosphorus single layers of $\approx 1.3 - 1.76$ eV[19,24,25]. This could be partly ascribed to the different stoichiometry of the SiO_2 layers used as a substrate, which induces a shift in the emission because of the different dielectric constant of the surrounding medium.[38] To verify this hypothesis, we have transferred black phosphorus flakes onto a Si substrate covered by a thin (~ 2 nm) layer of native oxide. Such a substrate has a larger dielectric constant than the standard Si/SiO_2 substrates. Thus, the exciton binding energy is expected to be lower and the emission energy should be blue shifted. A typical μPL spectrum of a flake transferred onto a Si substrate is shown in Fig. 2(a). While the main spectral features resemble those of a

flake on a Si/SiO_2 substrate, there is a large shift of the emission energy of ~ 80 meV. This confirms the dependence of the emission energy on the dielectric environment, in agreement with previous results.[10,27] The effect of the dielectric environment seems to be stronger than for atomically thin TMDs, in agreement with theory and experiment.[39]

In the spectrum measured on a standard Si/SiO_2 substrate, in addition to the neutral exciton recombination, we observed additional features at ~ 1.84 eV, which can be attributed to charged exciton recombination (systematically present in all the investigated flakes)[25] together with a low energy peak, typically at ~ 1.72 eV, and possibly related to excitons bound to impurities. The low energy feature is not always present, see *e.g.* the µPL spectrum on a Si substrate in Fig. 2(a).

Because of the low symmetry of the crystal structure and the screening in black phosphorus,[11,40] the exciton wave function is expected to be squeezed along the armchair direction, resulting in a polarization dependent PL emission.[24] The linear polarization dependence of the emission of our flakes was investigated by mounting polarizers/analyzers in both the excitation and the detection paths. Regardless of the polarization of the excitation beam, whenever the analyzer in the detection path was set to vertical (V), the intensity of the detected signal was a maximum, which is consistent with the strongly anisotropic nature of the exciton in black phosphorus[24]. For example, in Fig. 2(b), we show µPL spectra excited with a horizontally (H) polarized laser light and detected with either H or V direction of the analyzer. Moreover, for any fixed orientation of the analyzer in the detection path, the detected signal is always stronger when the analyzer in the excitation path was set to the H direction. This stems from the polarization dependent absorption properties of black phosphorus[16].

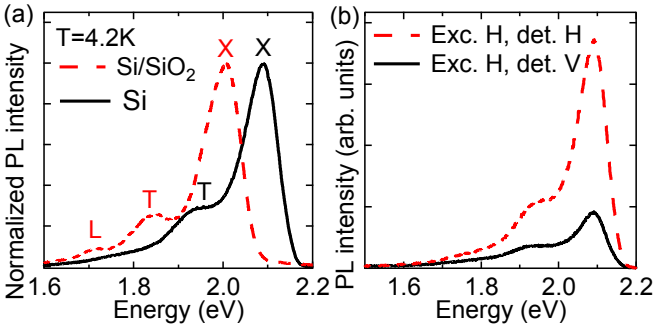

FIG. 2. (Color online) (a) Low temperature µPL spectra of black phosphorus flakes on Si/SiO_2 and Si substrates. X labels the neutral exciton transition, T the charged exciton and L the localized exciton. (b) Polarization resolved µPL spectra of a black phosphorus flake on Si/SiO_2.

The evolution of the µPL spectra as a function of the excitation power gives information concerning the nature of the observed transition lines. We have measured the power dependence of the µPL spectra for several black phosphorus monolayer flakes. In Fig. 3(a) we show representative spectra measured at low, intermediate, and high excitation powers P at $T = 4.2$ K. Even after exciting with $P > 1$ mW, the emission efficiency did not decrease for any of the investigated samples, suggesting that our preparation method helps improve the stability of the exfoliated black phosphorus flakes. Two peaks appear in the spectra of Fig. 3(a) for all excitation powers used. The neutral exciton peak slightly blue shifts at high excitation powers ($\lesssim 2$ meV), possibly due to a localized heating effect induced by the high power of the incoming laser beam (see also below for a discussion of temperature dependence of the black phosphorus PL).

In Fig. 3(b) we present the dependence of the integrated PL intensity of neutral and charged excitons as a function of the excitation power. At low excitation power, both intensities increase linearly with the power, as demonstrated by the fits to the power law $I \propto P^n$, with $n = 0.97 \pm 0.03$ for the neutral exciton and $n = 0.93 \pm 0.03$ for the charged exciton. At higher excitation power (not shown), both excitonic lines saturate at approximately the same level of excitation power ($P = 1$ mW), confirming that the two observed transitions are related to the recombination of a single electron-hole pair.

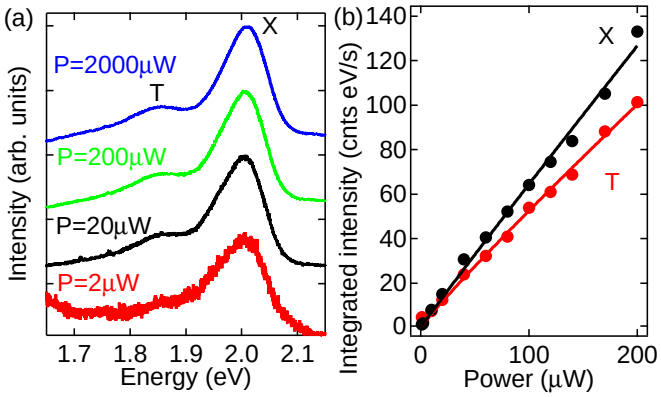

FIG. 3. (Color online) (a) µPL spectra of a black phosphorus single layer measured at different excitation powers. (b) Integrated intensity of the charged (T) and neutral (X) exciton emission versus excitation power. The solid lines are fits to a power law described in the text.

In view of the potential use of black phosphorus in a wide variety of electronic and optoelectronic applications, we have investigated the temperature dependence of its optical properties. In Fig. 4(a) we show normalized µPL spectra measured at different temperatures. With increasing temperature the charged exciton peak broadens. The neutral exciton emission blue shifts (measured $dE_g/dT \sim 3.1 \times 10^{-4}$ eV/K between 40 K and 160 K), which is consistent with earlier reports of the temperature dependence of the band gap of bulk black phosphorus ($dE_g/dT = 2.8 \times 10^{-4}$ eV/K[2]

or 2.33×10^{-4} eV/K[41]). The behavior of the emission energy of the excitonic peak is shown more in detail in Fig. 4(b). In bulk semiconductors, the variation of the band gap as a function of the temperature is direct consequence of the renormalization of the band gap via the electron-phonon interaction and of the thermal expansion of the lattice.[42] In general, the resulting effect is a decrease of the band gap with increasing temperature. Exceptions to this general behavior include lead salts[43–45] and copper halides.[46,47] While the role of thermal expansion[48] is often neglected[45], a variety of approaches has been proposed to fit the temperature dependence of the band gap[49], which sometimes fail to provide physical insight for the extracted fitting parameters. A more useful approach to the fit the temperature dependence of the band gap requires in principle the knowledge of the details of the phonon density of states and of the electron-phonon coupling constants, which makes this treatment somewhat cumbersome. In a simplified approach, the essential features of the electron-phonon interaction are accounted for by considering contributions only at energies where the phonon density of states displays sharp peaks (two-oscillator model).[45,47,50,51] In this framework, the band gap E_g is approximated by

$$E_g(T) = E_0 + E_1 \left(\frac{2}{e^{\frac{\hbar\omega_1}{k_B T}} - 1} + 1 \right) + E_2 \left(\frac{2}{e^{\frac{\hbar\omega_2}{k_B T}} - 1} + 1 \right),$$

where E_0 is the bare band gap (i.e. the low temperature band gap exhibited in the absence of zero point motion), $E_1 + E_2$ is the renormalization energy and $\hbar\omega_1 = 17.23$ meV and $\hbar\omega_2 = 52.82$ meV denote the two oscillator energies, as extracted from the computed phonon density of states of monolayer black phosphorus.[52] The neutral exciton emission energy is then given by $E_g(T) - E_X$, where E_X is the exciton binding energy . The solid curve shown in Fig. 4(b) is obtained by fitting the experimental data, yielding $(E_0 - E_X) = 2.22 \pm 0.02$ eV (larger than the observed low T transition energy, suggesting the occurrence of band gap renormalization due to electron-phonon interaction), $E_1 = 72.6 \pm 0.3$ meV, and $E_2 = -297 \pm 3$ meV.

The integrated intensity $I(T)$ of the excitonic transition as a function of the inverse substrate temperature T^{-1} is shown in Fig. 4(c). With increasing temperature, the emission intensity decreases, owing to the thermal activation of non-radiative recombination centers. To quantify the activation energy E_A, the experimental data is fitted using $I(T)/I(T=0) = 1/(1 + a\, e^{-E_A/k_B T})$,[53] where a is related to the ratio of the radiative and non-radiative lifetimes,[54] to give $E_A = 10 \pm 1$ meV, and $a = 6.8 \pm 2$. The significantly lower value of E_A as compared to the computed exciton binding energy[10] confirms that the decrease of the PL intensity at high T is brought about by the thermal occupation of non radiative recombination centers rather than the dissociation of the excitons.

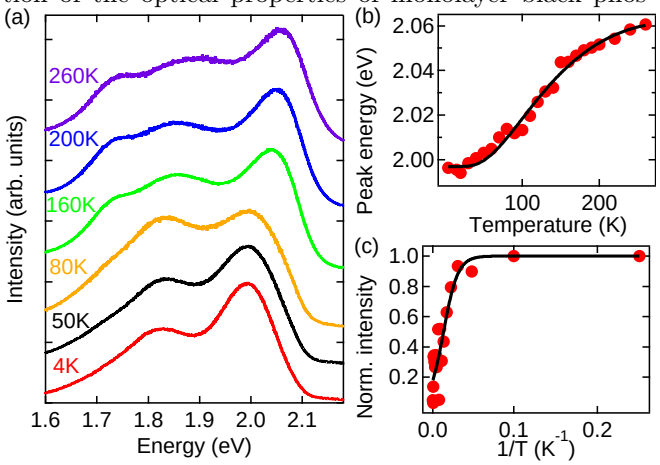

FIG. 4. (Color online) (a) μPL spectra of a black phosphorus single layer measured at different temperatures. (b) Emission energy of the neutral exciton as a function of the temperature. (c) Integrated intensity of the neutral exciton versus temperature. The solid lines are fits to the models described in the text.

In summary, we have performed a detailed investigation of the optical properties of monolayer black phosphorus mechanically exfoliated in an Ar atmosphere. No significant degradation of the PL emission was induced by the laser illumination, suggesting that this preparation method preserves the optical properties of the black phosphorus flakes. The shift of the Raman modes measured on the exfoliated flakes with respect to the bulk black phosphorus confirms the single layer character of the exfoliated black phosphorus flakes. The measured μPL spectra exhibit strong emission lines, attributed to the recombination of neutral and charged excitonic complexes. The large emission energy observed as compared to the previously reported values[19,24,25] is a further proof of the single layer character of the investigated flakes, consistently with an increased quantum confinement with a decreasing number of layers[11]. The excitonic nature of the observed PL was confirmed by the observed polarization dependence and by the nearly linear increase of the emission intensity with the excitation power. The increase in the emission energy with temperature was modeled with a two-oscillator model to account for the temperature dependence of semiconductor band gap.

ACKNOWLEDGMENTS

The authors gratefully acknowledge Baptiste Vignolle for his assistance with the glove box and for his careful proof reading and Geert Rikken for providing the bulk black phosphorus. AAM acknowledges financial support from the French foreign ministry. This work was partially supported by ANR JCJC project milliPICS, the Region Midi-Pyrénées under contract MESR 13053031 and STCU project 5809.

* Present address: High Field Magnet Laboratory (HFML-EMFL), Institute for Molecules and Materials, Radboud University, Toernooiveld 7, 6525 ED Nijmegen, The Netherlands
† paulina.plochocka@lncmi.cnrs.fr

[1] R. W. Keyes, Physical Review **92**, 580 (1953).
[2] D. Warschauer, Journal of Applied Physics **34**, 1853 (1963).
[3] Y. Maruyama, S. Suzuki, K. Kobayashi, and S. Tanuma, Physica B+C **105**, 99 (1981).
[4] H. Asahina, Y. Maruyama, and A. Morita, Physica B+C **117118, Part 1**, 419 (1983).
[5] J. C. Jamieson, Science **139**, 1291 (1963).
[6] J. Wittig and B. T. Matthias, Science **160**, 994 (1968).
[7] S. Sugai and I. Shirotani, Solid State Communications **53**, 753 (1985).
[8] S. Narita, S. Terada, S. Mori, K. Muro, Y. Akahama, and S. Endo, Journal of the Physical Society of Japan **52**, 3544 (1983).
[9] Y. Takao, H. Asahina, and A. Morita, Journal of the Physical Society of Japan **50**, 3362 (1981).
[10] A. Castellanos-Gomez, L. Vicarelli, E. Prada, J. O. Island, K. L. Narasimha-Acharya, S. I. Blanter, D. J. Groenendijk, M. Buscema, G. A. Steele, J. V. Alvarez, H. W. Zandbergen, J. J. Palacios, and H. S. J. van der Zant, 2D Materials **1**, 025001 (2014).
[11] V. Tran, R. Soklaski, Y. Liang, and L. Yang, Physical Review B **89**, 235319 (2014).
[12] X. Ling, H. Wang, S. Huang, F. Xia, and M. S. Dresselhaus, Proceedings of the National Academy of Sciences **112**, 4523 (2015).
[13] K. S. Novoselov, A. K. Geim, S. V. Morozow, D. Jiang, M. I. Katsnelson, I. V. Grigorieva, S. V. Dubonos, and A. A. Firsov, Nature **438**, 197 (2005).
[14] Q. H. Wang, K. Kalantar-Zadeh, A. Kis, J. N. Coleman, and M. S. Strano, Nature Nanotechnology **7**, 699 (2012).
[15] T. Low, A. S. Rodin, A. Carvalho, Y. Jiang, H. Wang, F. Xia, and A. H. Castro Neto, Physical Review B **90**, 075434 (2014).
[16] F. Xia, H. Wang, and Y. Jia, Nature Communications **5**, 4458 (2014).
[17] J. Qiao, X. Kong, Z.-X. Hu, F. Yang, and W. Ji, Nature Communications **5**, 4475 (2014).
[18] L. Li, Y. Yu, G. J. Ye, Q. Ge, X. Ou, H. Wu, D. Feng, X. H. Chen, and Y. Zhang, Nature Nanotechnology **9**, 372 (2014).
[19] H. Liu, A. T. Neal, Z. Zhu, Z. Luo, X. Xu, D. Tománek, and P. D. Ye, ACS Nano **8**, 4033 (2014).
[20] M. Buscema, D. J. Groenendijk, S. I. Blanter, G. A. Steele, H. S. J. van der Zant, and A. Castellanos-Gomez, Nano Letters **14**, 3347 (2014).
[21] S. P. Koenig, R. A. Doganov, H. Schmidt, A. H. Castro Neto, and B. Özyilmaz, Applied Physics Letters **104**, 103106 (2014).
[22] Z. X. Gan, L. L. Sun, X. L. Wu, M. Meng, J. C. Shen, and P. K. Chu, Applied Physics Letters **107**, 021901 (2015).
[23] S. Zhang, J. Yang, R. Xu, F. Wang, W. Li, M. Ghufran, Y.-W. Zhang, Z. Yu, G. Zhang, Q. Qin, and Y. Lu, ACS Nano **8**, 9590 (2014).
[24] X. Wang, A. M. Jones, K. L. Seyler, V. Tran, Y. Jia, H. Zhao, H. Wang, L. Yang, X. Xu, and F. Xia, Nature Nanotechnology **10**, 517 (2015).
[25] J. Yang, R. Xu, J. Pei, Y. W. Myint, F. Wang, Z. Wang, S. Zhang, Z. Yu, and Y. Lu, Light-Science & Applications **4**, e312 (2015).
[26] L. Liang, J. Wang, W. Lin, B. G. Sumpter, V. Meunier, and M. Pan, Nano Letters **14**, 6400 (2014).
[27] A. H. Woomer, T. W. Farnsworth, J. Hu, R. A. Wells, C. L. Donley, and S. C. Warren, ACS Nano **9**, 8869 (2015).
[28] C. Lee, H. Yan, L. E. Brus, T. F. Heinz, J. Hone, and S. Ryu, ACS Nano **4**, 2695 (2010).
[29] H. R. Gutirrez, N. Perea-Lpez, A. L. Elas, A. Berkdemir, B. Wang, R. Lv, F. Lpez-Uras, V. H. Crespi, H. Terrones, and M. Terrones, Nano Letters **13**, 3447 (2013).
[30] H. Li, Q. Zhang, C. C. R. Yap, B. K. Tay, T. H. T. Edwin, A. Olivier, and D. Baillargeat, Advanced Functional Materials **22**, 1385 (2012).
[31] S.-L. Li, H. Miyazaki, H. Song, H. Kuramochi, S. Nakaharai, and K. Tsukagoshi, ACS Nano **6**, 7381 (2012).
[32] A. C. Ferrari, J. C. Meyer, V. Scardaci, C. Casiraghi, M. Lazzeri, F. Mauri, S. Piscanec, D. Jiang, K. S. Novoselov, S. Roth, and A. K. Geim, Physical Review Letters **97**, 187401 (2006).
[33] A. Gupta, G. Chen, P. Joshi, S. Tadigadapa, and Eklund, Nano Letters **6**, 2667 (2006).
[34] S. Sugai, T. Ueda, and K. Murase, Journal of the Physical Society of Japan **50**, 3356 (1981).
[35] A. Favron, E. Gaufres, F. Fossard, A.-L. Phaneuf-L'Heureux, N. Y.-W. Tang, P. L. Levesque, A. Loiseau, R. Leonelli, S. Francoeur, and R. Martel, Nature Materials **14**, 826 (2015).
[36] X. Luo, X. Lu, G. K. W. Koon, A. H. C. Neto, B. Özyilmaz, Q. Xiong, and S. Y. Quek, Nano Letters **15**, 3931 (2015).
[37] W. Lu, H. Nan, J. Hong, Y. Chen, C. Zhu, Z. Liang, X. Ma, Z. Ni, C. Jin, and Z. Zhang, Nano Research **7**, 853 (2014).
[38] J. H. Choi and M. S. Strano, Applied Physics Letters **90**, 3114 (2007).
[39] Y. Lin, X. Ling, L. Yu, S. Huang, A. L. Hsu, Y.-H. Lee, J. Kong, M. S. Dresselhaus, and T. Palacios, Nano Letters **14**, 5569 (2014).
[40] P. Li and I. Appelbaum, Physical Review B **90**, 115439 (2014).
[41] M. Baba, Y. Nakamura, K. Shibata, and A. Morita, Japanese Journal of Applied Physics **30**, L1178 (1991).
[42] M. Cardona and M. L. W. Thewalt, Reviews of Modern Physics **77**, 1173 (2005).
[43] R. A. Laff, Journal of Applied Physics **36**, 3324 (1965).
[44] Q. Dai, Y. Zhang, Y. Wang, M. Z. Hu, B. Zou, Y. Wang, and W. W. Yu, Langmuir **26**, 11435 (2010).
[45] P. Dey, J. Paul, J. Bylsma, D. Karaiskaj, J. M. Luther, M. C. Beard, and A. H. Romero, Solid State Communications **165**, 49 (2013).
[46] A. Göbel, T. Ruf, M. Cardona, C. T. Lin, J. Wrzesinski, M. Steube, K. Reimann, J.-C. Merle, and M. Joucla, Physical Review B **57**, 15183 (1998).
[47] M. Cardona and R. K. Kremer, Thin Solid Films **571**, 680 (2014).
[48] P. B. Allen and M. Cardona, Physical Review B **27**, 4760 (1983).
[49] K. P. ODonnell and X. Chen, Applied Physics Letters **58**, 2924 (1991).
[50] L. Viña, S. Logothetidis, and M. Cardona, Physical Re-

view B **30**, 1979 (1984).
[51] H. J. Lian, A. Yang, M. L. W. Thewalt, R. Lauck, and M. Cardona, Physical Review B **73**, 233202 (2006).
[52] Y. Aierken, D. Çakır, C. Sevik, and F. M. Peeters, Physical Review B **92**, 081408 (2015).
[53] M. Leroux, N. Grandjean, B. Beaumont, G. Nataf, F. Semond, J. Massies, and P. Gibart, Journal of Applied Physics **86**, 3721 (1999).
[54] Y. Fang, L. Wang, Q. Sun, T. Lu, Z. Deng, Z. Ma, Y. Jiang, H. Jia, W. Wang, J. Zhou, and H. Chen, Scientific Reports **5**, 12718 (2015).